

Low Loss Gears

Bernd-Robert Höhn, Klaus Michaelis,
Albert Wimmer

This article is printed with permission of the copyright holder, the American Gear Manufacturers Association, 500 Montgomery St., Alexandria, VA 22314-1560. Statements presented in this paper are those of the authors and may not represent the position or opinion of the AMERICAN GEAR MANUFACTURERS ASSOCIATION.

Management Summary

In most transmission systems, one of the main power loss sources is the loaded gear mesh. High power losses lead to high energy consumption, high temperatures, early oil aging, increased failure risk and high cooling requirements. In many cases, high efficiency is not the main focus, and design criteria such as load capacity or vibration excitation predominate the gear shape design. Those design criteria mostly counteract the highest possible efficiency. In this article, the influences of gear geometry parameters on gear efficiency, load capacity, and excitation are shown. Therefore, design instructions can be derived, which lead to low-loss gears with equivalent load capacity

Introduction

Power losses occur in different components of a gearbox. Each gearbox element produces some power losses. The total power loss is the sum of the power losses of the single elements. Basic gearbox elements are bearings,

gears and seals. Their power losses are usually individually mentioned. Other potentially integrated elements, such as clutches or oil pumps, also produce losses, but these are not usually treated separately. Their power losses are merged in auxiliaries. According to their types, losses can be further divided into no-load losses and load-dependent losses. Equation 1 (on page 29) shows the summation of all power losses P_v in a typical gearbox. Losses in bearings and gears usually predominate in a gearbox.

No-load losses comprise all losses that exist when a gearbox is rotating, but not transmitting power. No-load losses derive from seals or from windage and churning.

Load-dependent losses occur only in elements that carry the transmitted power or portions of it, such as bearings and gears. They encompass all power losses that vary with the power transmission in the concerned element. They evolve when two surfaces under

pressure move relative to each other. Power losses in this case depend on the acting force between the solids, the sliding speed, and on the coefficient of friction established in the contact of the surfaces.

For the composition of total power losses P_v in a gearbox, the following four main components are investigated:

- No-load power losses in bearings
- Load-dependent power losses in bearings
- No-load power losses in gears
- Load-dependent power losses in gears

The investigations are based on calculations for which the FVA-software *WTplus*, *STplus* and *RIKOR* are used (Refs. 1, 10 and 13).

Gearing Model

For the calculations, a gearing model is necessary. The data of the gear set that was used for the calculation were taken from an existing gear set of one of our test gearboxes. Figure 1 (overleaf) shows the main data of the reference gearbox model and a transverse section of the reference gear shape on which the calculations are based. Starting from that, single gearing modifications are applied in order to investigate the influence of each single parameter.

Power Loss Portions

In Figure 2, the amount of power losses for each of the four considered components is depicted versus the rotational speed at the operating conditions given in Figure 1. The investigation of power loss composition in Figure 2 is accomplished with the example of modified reference gearing with spur gears ($\beta = 0^\circ$). It shows that the gear no-load losses increase progressively with speed, while the other components seem to depend fairly linearly on the speed. For the vast range of rotational speeds, the main portion of losses are load-dependent gear losses. Only for very high speeds do no-load losses prevail, though the load-dependent gear losses may still occupy an important portion. Bearing losses have only subordinate portions of the total losses

Prof. Dr.-Ing. Bernd-Robert Höhn is head of the Institute of Machine Elements and the Gear Research Centre FZG at the Technical University Munich. He worked for 10 years at Audi as manager of the departments for gear research, design and experimental investigations and became a professor in 1989.

Dr.-Ing. Klaus Michaelis is research group manager at the FZG. His main working areas are load carrying capacity and experimental tribology of cylindrical, bevel and worm gears.

Dr.-Ing. Albert Wimmer was assistant at the FZG. The subject of his PhD thesis was theoretical and experimental investigation of load dependent losses in gears. He is now working with Weigl Engineering GmbH in the field of innovation management of geared systems.

throughout the whole speed range.

In addition, the sum of these losses is rated against the power transmission, which results in the loss degree ζ , the complement of the degree of efficiency η :

$$\zeta = \frac{P_V}{P_{in}} = 1 - \eta \quad (2)$$

with P_V total power loss (measured in watts), P_{in} input power (measured in watts), η degree of efficiency.

The loss degree ζ shows a significant minimum between 10 and 20 m/s rotational speed. This reflects the basic changes in the coefficient of friction in the mating gears from the mixed lubrication regime for low speeds towards elasto-hydrodynamic (EHD) friction at higher speeds. Depending on the geometry of the transmission and the operating conditions, this minimum occurs at different speed ranges.

The prevailing power loss portion is very dependent on the operating conditions. However, in order to minimize the power losses, a focus must always be set onto load-dependent gear losses since their portion is always significant. With increasing speed, no-load losses of gears need to be considered increasingly.

Basics of Load-Dependent Gear Losses

The load-dependent losses depend on both gear and lubricant properties. The calculation of load-dependent power losses in gears is based on the law of friction according to Coulomb (Ref. 3).

$$F_R = \mu \cdot F_N \quad (3)$$

$$P_{VP} = F_R \cdot v_g = \mu \cdot F_N \cdot v_g \quad (4)$$

with F_R friction force (measured in Newtons), μ coefficient of friction, F_N normal force (measured in Newtons), P_{VP} load-dependent power loss (measured in Watts), v_g sliding speed (m/s).

Equation 4 is valid for a single point of contact. In order to receive the mean power loss of two mating

$$\begin{array}{c} \text{Index} \qquad \qquad \text{Z: gears} \qquad \qquad \text{L: bearings} \qquad \qquad \text{D: seals} \qquad \qquad \text{X: auxiliaries} \\ P_V = P_{VZ0} + P_{VZP} + P_{VL0} + P_{VLP} + P_{VD} + P_{VX} \\ \downarrow \qquad \qquad \downarrow \qquad \qquad \downarrow \qquad \qquad \downarrow \qquad \qquad \downarrow \\ \text{0: no-load} \\ \text{P: load dependent} \end{array}$$

Equation 1.

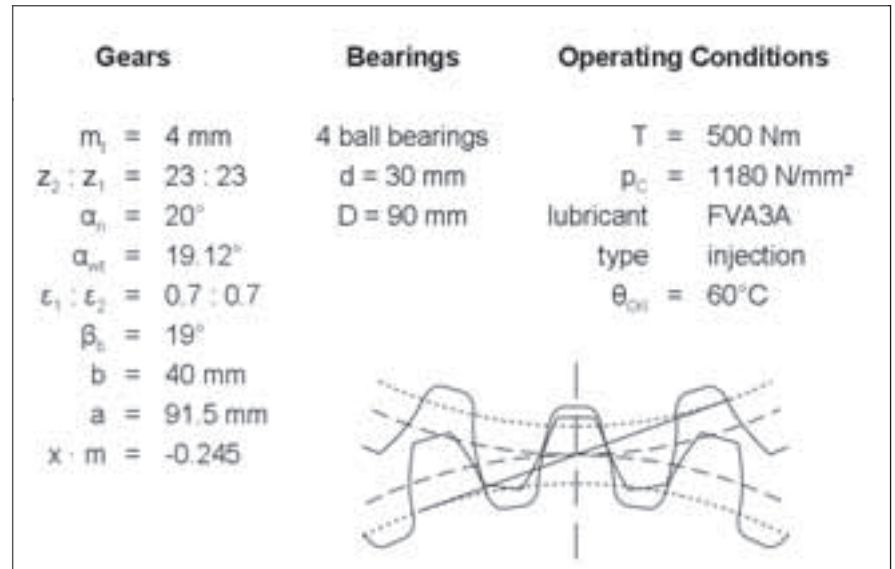


Figure 1—Main data of reference gearing model and gear cross section.

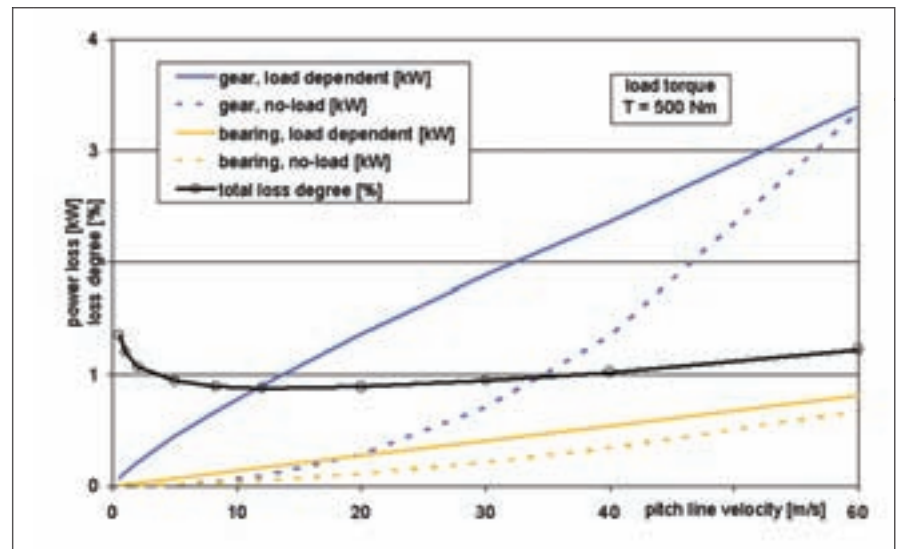


Figure 2—Power loss composition in the model gearbox vs. pitch line velocity.

gears, all points of contact along the path of contact need to be considered. The power loss is calculated by the integral of the product of sliding speed, coefficient of friction and load over the path of contact.

$$P_{VZP} = \frac{1}{p_{et}} \int_A^E P_{VZP}(x) dx \quad (5)$$

with p_{et} transverse base pitch (measured

in mm), \overline{AE} path of contact (measured in mm).

All three parameters (coefficient of friction, normal load, sliding speed) vary along the path of contact (Fig. 3).

Sliding speed is a geometry parameter that is derived from the gear shape and can be calculated exactly.

The load distribution along the path of contact can be approximately set to

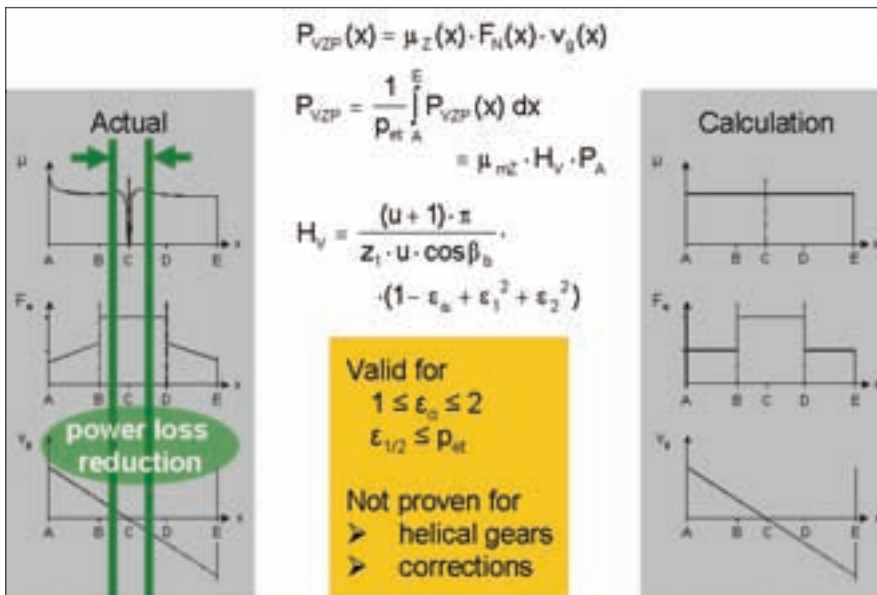


Figure 3—Tribological conditions along the path of contact.

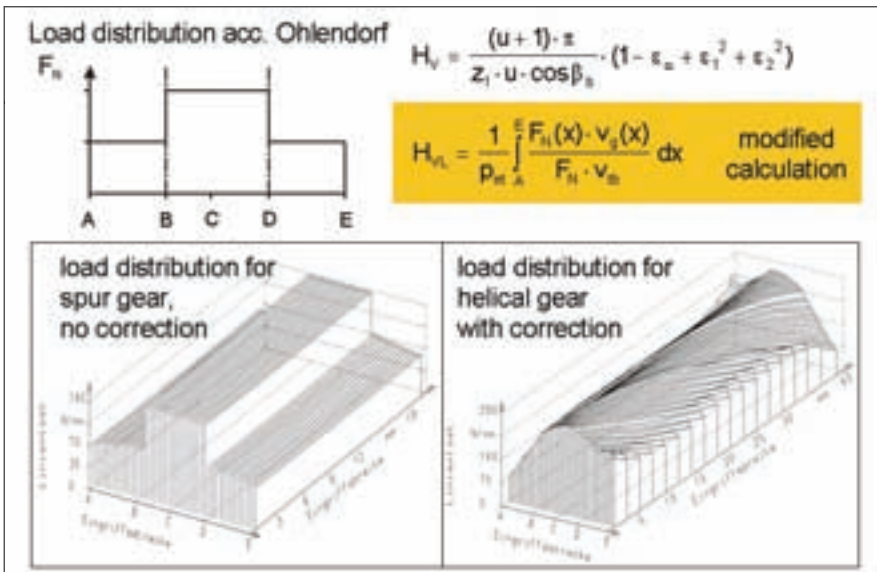


Figure 4—Gear loss factors H_V and H_{VL} .

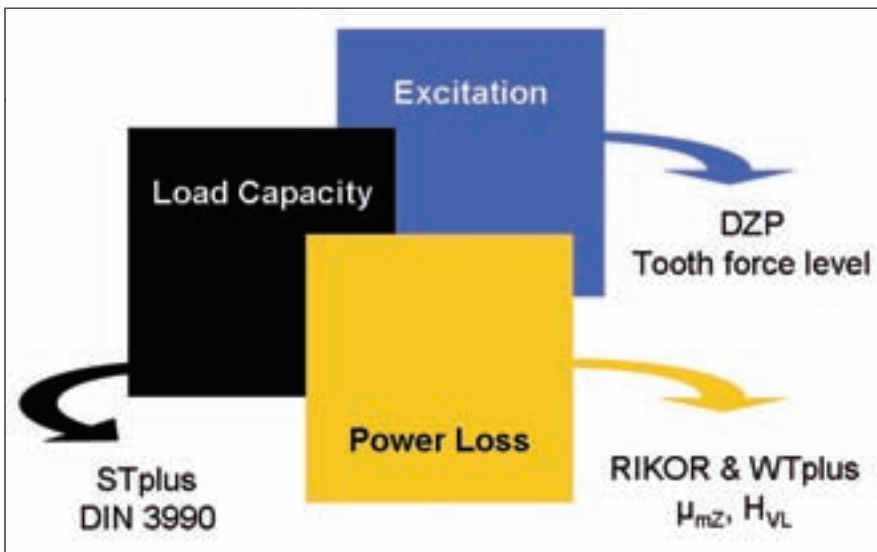


Figure 5—Calculation methods for different parameters.

the total load resulting from the torque and split up into the number of pairs of teeth in contact. This assumption is a simplistic approximation (Ref. 9). The coefficient of friction over the path of contact is assumed to be approximately constant. At the pitch point C, where sliding is zero and pure rolling occurs, the instantaneous drop of the coefficient of friction to zero has to be considered. This deviation of the coefficient of friction takes place where the sliding speed is zero. Hence, in the integral, this deviation is negligible. The coefficient of friction is approximated according to the FVA project No. 166, done by Schlenk (Ref. 11), with the following equation:

$$\mu_{mZ} = 0.048 \cdot \left(\frac{F_{tb}/b}{v_{\Sigma C} \cdot \rho_{redC}} \right)^{0.2} \cdot \eta_{oil}^{-0.05} \cdot Ra^{0.25} \cdot X_L \quad (6)$$

with μ_{mZ} mean coefficient of friction, F_{tb} circumferential force at base circle (measured in newtons), $v_{\Sigma C}$ sum speed at operating pitch circle (m/s), ρ_{redC} reduced radius of curvature at pitch point (mm), η_{oil} dynamic oil viscosity at oil temperature (mPas), Ra arithmetic mean roughness (μm), X_L factor for oil type.

With the introduced simplifications (constant coefficient of friction along the path of contact, equal load distribution onto mating pairs of teeth), Equation 4 can be applied to gears and transformed into Equation 7:

$$P_{VZP} = \mu_{mZ} \cdot H_V \cdot P_A \quad (7)$$

with H_V gear loss factor:

See page 31 for Equation (8)

with $u = z_2/z_1$ gear ratio, z number of teeth (1 pinion, 2 wheel gear), β_b base helix angle ($^\circ$),

$$\epsilon_a = \frac{\overline{AE}}{p_{et}} \text{ transverse contact ratio,}$$

$$\epsilon_1 = \frac{\overline{CE}}{p_{et}} \text{ addendum contact ratio of pinion,}$$

$\varepsilon_2 = \frac{\overline{AC}}{P_{et}}$ addendum contact ratio of wheel gear.

The gear loss factor H_V was introduced by Ohlendorf (Ref. 9) and is only dependent on gear geometry.

These equations were set up for usual spur gear geometries ($1 \leq \varepsilon_\alpha \leq 2$ and $\varepsilon_{1/2} \leq \rho_{et}$) and produce acceptable results in these cases. Extreme gear shapes, however, may result in calculated power losses, which deviate significantly from actual power losses. By more detailed considerations, a better approximation of the real distribution of the load along the path of contact can be obtained by using sophisticated calculation methods such as FEM or the FVA-program *RIKOR*. This is proven by experimental investigations (Ref. 14). Gear loss factors based on such methods are called local gear loss factors H_{VL} . Differences between H_V and H_{VL} are significant for high-contact-ratio gears, helical gears or gears with profile corrections (Fig. 4).

The gear loss factors H_V or H_{VL} , respectively, comprise the integral of the product of the sliding speed and the load distribution (Refs. 9, 14). Here—for the calculation of load-dependent power losses of gears—the local gear loss factor H_{VL} with the more realistic load distribution according to the FVA-program *RIKOR* is used (Ref. 10).

For gear design, power losses are often of subordinate interest, compared to load capacity and excitation level. So, if gears are to be optimized in terms of efficiency, load capacity and excitation must not be neglected. To evaluate single gear geometry parameters and their influence on power loss, load capacity and excitation are investigated by the means of FVA-programs according to Figure 5. Excitation is evaluated by the tooth force level, which represents the dynamic load in the tooth contact without respect to the further environment. This load dynamics is the cause of, but not equal to, real load dynamics, vibration and noise.

Lubricant properties affect the power losses via the coefficient of friction μ and are not subject to this investigation. Their influence is supposed to

$$H_V = \frac{(u+1) \cdot \pi}{z_1 \cdot u \cdot \cos(\beta_b)} \cdot (1 - \varepsilon_\alpha + \varepsilon_1^2 + \varepsilon_2^2)$$

Equation 8.

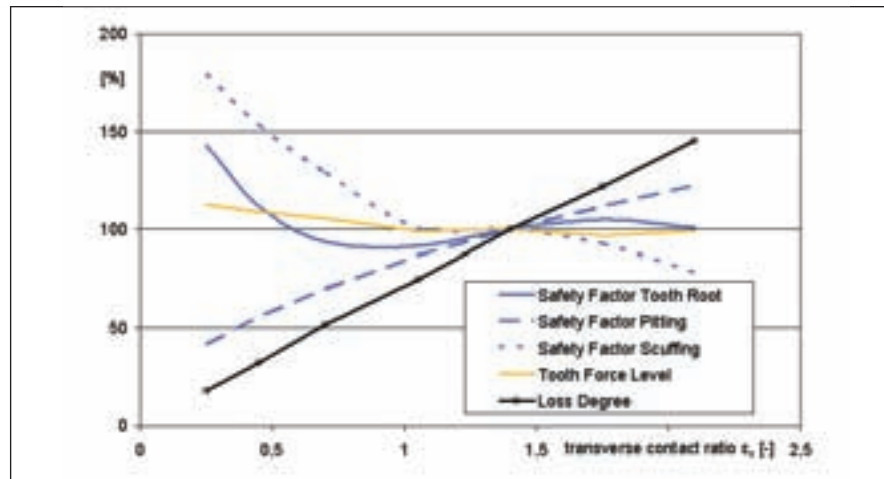


Figure 6—Influence of transverse contact ratio on power loss and load capacities.

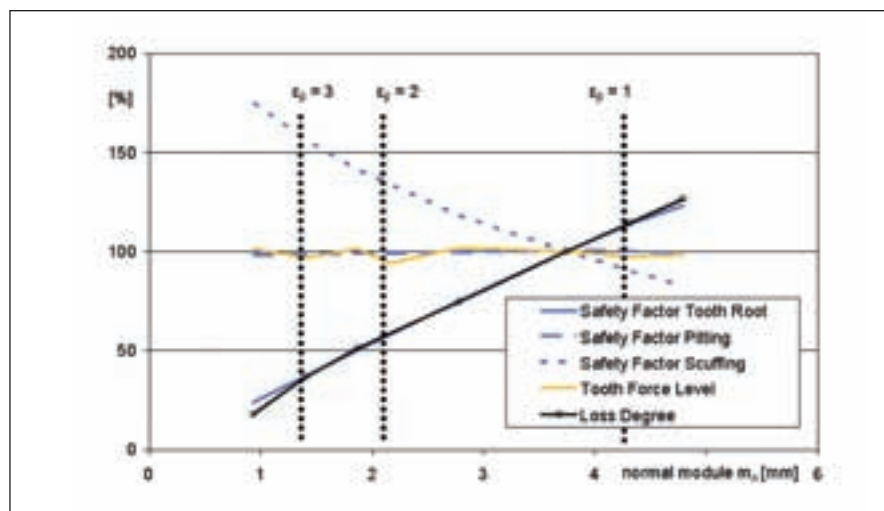


Figure 7—Influence of module on power loss and load capacities.

be constant here.

Influence of Gearing Geometry on Load-Dependent Power Losses

Figures 6–13 show the influences of gear geometry parameters on the gear load-dependent power losses compared to the reference gears given in Figure 1. The influence of these parameters on the coefficient of friction is included. For these parameter variations, the pitting and tooth fracture capacities are provided referring to the reference gearing with capacities of 100%. Ideally, power loss and tooth force level are low while the safety factors of load capacities are high.

The most important geometric parameters are transverse contact ratio (Fig. 6) and module size (Fig. 7). Less strong is the influence of the pressure angle, but its importance comes from the advantage that, in the given range, a higher pressure angle has only advantageous effects both on power loss reduction and higher load capacities, and no unfavorable effects on excitation (Fig. 8).

With helix angle, power losses increase generally but to a limited extent (Fig. 9). For minimum power losses with small transverse contact ratio, there has to be a significant over-

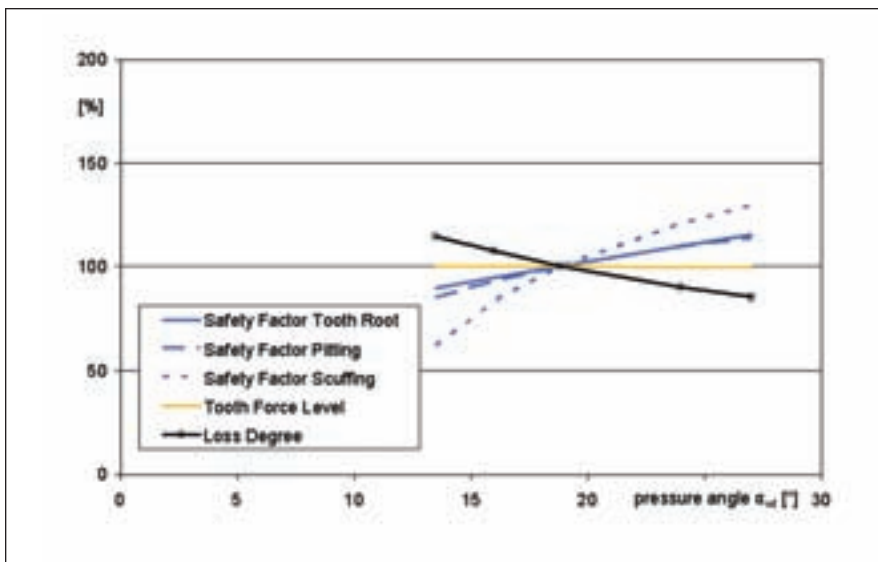


Figure 8—Influence of pressure angle on power loss and load capacities.

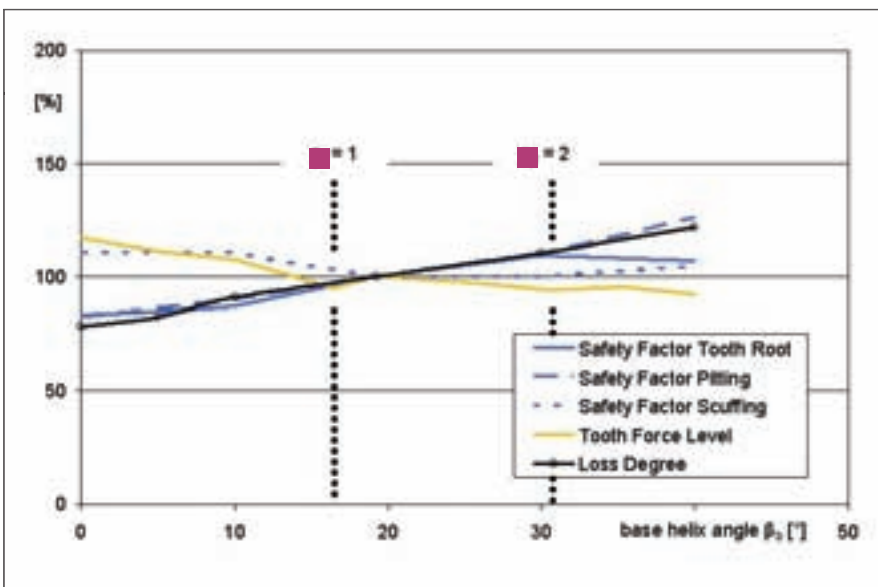


Figure 9—Influence of helix angle on power loss and load capacities.

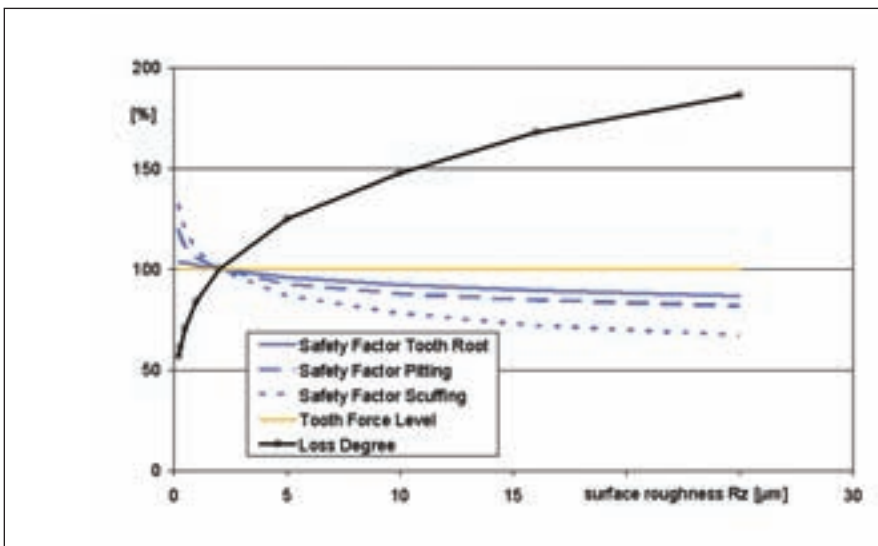


Figure 10—Influence of surface roughness on power loss and load capacities.

lap contact ratio ($\epsilon_\beta > 1$) for proper load capacity and noise excitation.

The influence of surface roughness shows positive effects if it is reduced (Fig. 10). Unfortunately, an improvement is usually subject to cost increase. Recent investigations show that this effect is limited. Below a certain roughness, there is no further improvement. Moreover, there are other effects of surface structure such as roughness orientation, which are not expressed by surface roughness but can affect the power loss to a substantial extent.

The gear ratio and face width parameters (at constant load per face width) are usually constraints that cannot be changed. Their effect on power loss, capacities, and excitation is shown in Figure 11 and Figure 13, respectively.

Addendum transverse contact ratio is best if equally split between both gears, but small deviations have marginal impact (Fig. 12).

Gearing Optimization Process

The following steps conclude the optimization process towards low-loss gears. Most of these steps are considered unconventional, but prove more efficient to the gear design with respect to power savings. However, it is not a unidirectional process, but rather a loop that has to be run through cyclically.

- Corrections for load reduction in areas of contacts with high sliding speed
- Reduction of module down to tooth root fracture limit
- Reduction of transverse contact ratio down to pitting capacity limit
- Tooth root fillet radius as large as possible
- Increase of pressure angle
- Increase of face width
- Helix angle for adequate overlap contact ratios

Power Loss Reduction with Optimized Gearing

From the reference gearing given in Figure 1, an optimized gearing is derived. It has the same or better load capacities, but lower power losses. Figure 14 compares the absolute figures of power loss components at

one operating point ($v_t = 10 \text{ m/s} \approx n = 2,100 \text{ U/min}$; load torque 500 Nm). In this example, the bearing type has been optimized, but is not relevant here. The main changes applied encompass the following:

Bearings

- Different type (ball/taper roller)
- Size ($d_m = 60 \text{ mm}/43.5 \text{ mm}$)

Gears

- Module reduction ($4 \text{ mm}/2 \text{ mm}$)
- Transverse pressure angle increase ($19.1^\circ/41.5^\circ$)
- Transverse contact ratio reduction ($1.4/0.6$)
- Face width increase ($40 \text{ mm}/80 \text{ mm}$)
- Overlap contact ratio increase ($1.18/4.73$)

For the optimized gears, the module and the transverse contact ratio are radically cut back, compensated by a doubled face width. So, the optimized gears have a low transverse contact ratio, but a high overlap ratio for the same load-carrying capacity. Furthermore, the tooth root fillet has a larger radius in order to support the tooth root fracture capacity, and the transverse pressure angle is significantly increased for a larger radius of curvature, which backs up the pitting capacity and results in a lower coefficient of friction. Total power losses can be reduced by two-thirds in total (68.8%), where the largest portion of loss reduction is achieved for the load-dependent gear losses (see Fig. 14). The reduction of load-dependent gear losses is caused by two advantageous effects: a lower coefficient of friction because of better curvature ($\mu_m = 0.030$; -32%) and lower gear loss factor ($H_{VL} = 0.045$; -78%). This combination results in a reduction of load-dependent gear losses of $[1 - (1 - 0.32) \cdot (1 - 0.78)] = 85\%$. In Figure 14, the transverse section of both the reference and the optimized gears is included.

A similar optimization procedure is applied to Type C gears, which is a frequently used test gear geometry for many kinds of gear and lubrication tests. In Figure 15, the main geometry parameters of Type C gears are given,

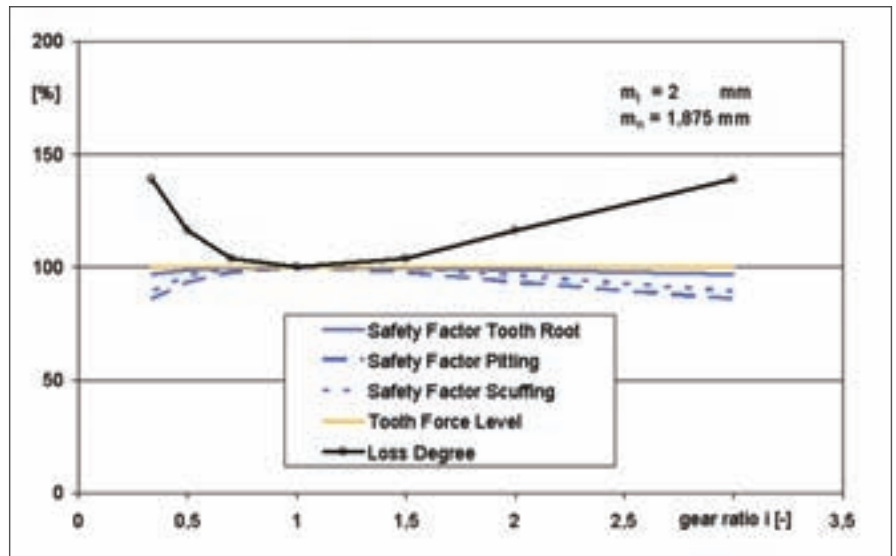


Figure 11—Influence of gear ratio on power loss and load capacities.

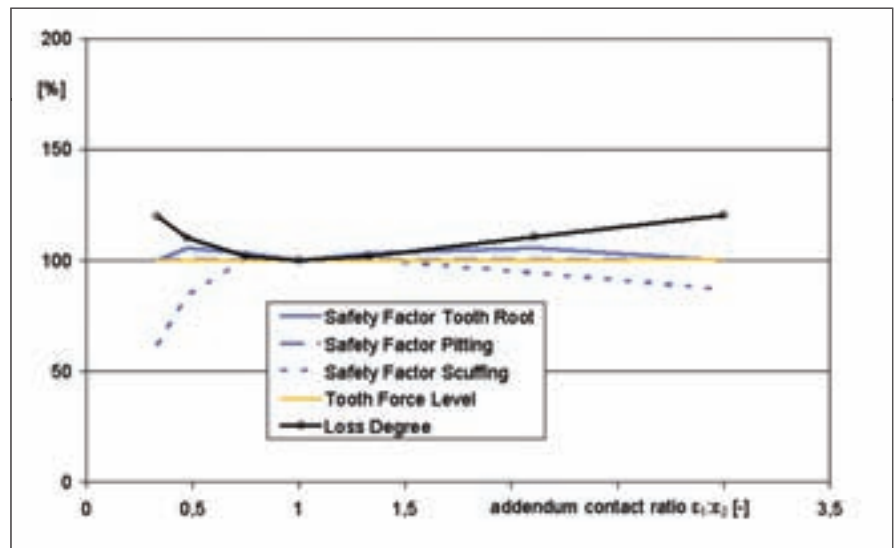


Figure 12—Influence of addendum contact ratio on power loss and load capacities.

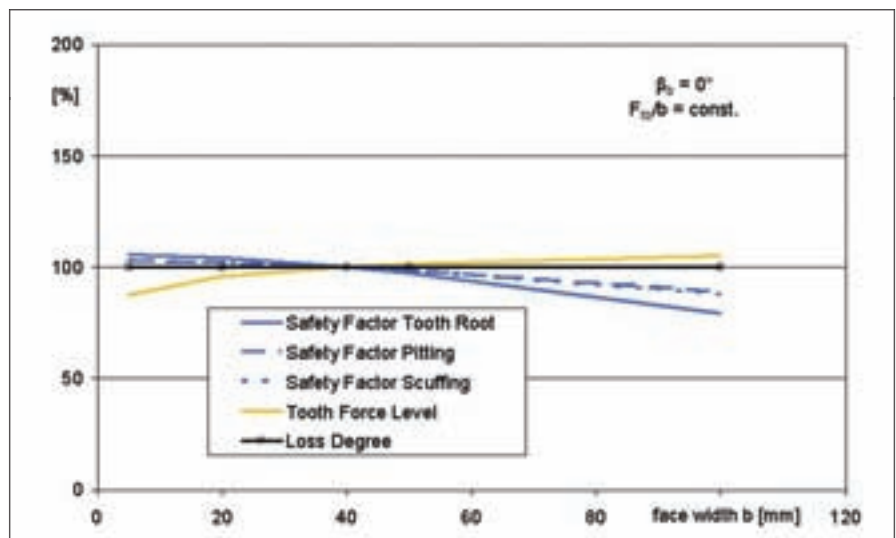


Figure 13—Influence of face width on power loss and load capacities.

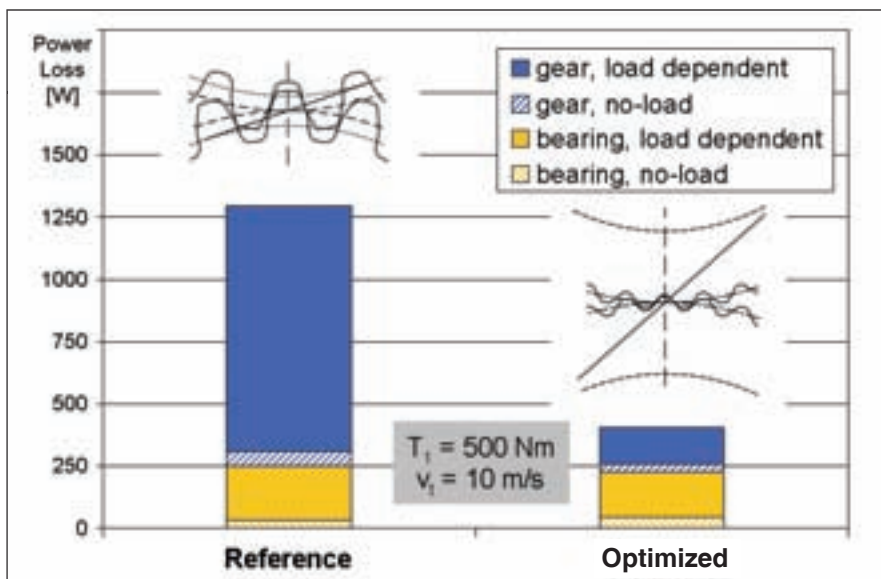


Figure 14—Comparison of power loss composition of reference and optimized gearing.

	Type C	Low Loss
m_n	4.5 mm	1.75 mm
$z_2 : z_1$	16 : 24	40 : 60
α_n	20°	40°
α_{ref}	22.4°	41.6°
$\epsilon_1 : \epsilon_2$	0.72 : 0.71	0.29 : 0.26
β_b	0°	15°
b	14 mm	20 mm
ρ_{add}	0.25	0.5
a	91.5 mm	91.5 mm
R_a	0.17 μm	0.38 μm
DIN 3990		
KS9		
$v_1 = 8.3 \text{ m/s}$		
FVA3A		
S_F	0.81 / 0.87	0.89 / 0.89
S_H	1.79 / 1.86	1.86 / 1.82
S_B	1.14	11.72

Figure 15—Gear geometry of Type C gears and corresponding low-loss gears.

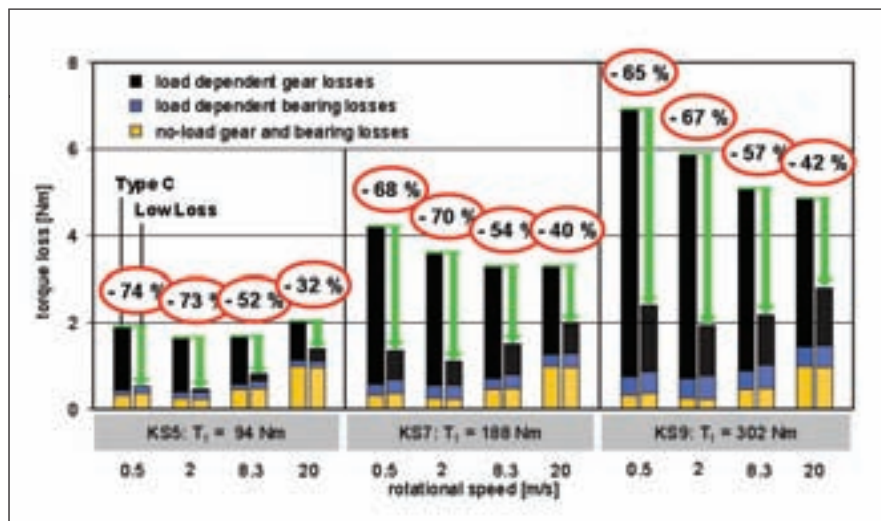


Figure 16—Experimental results of low-loss gears.

as well as those of the corresponding low-loss gears. Additionally, the calculated safety factors are shown. Those of low-loss gears are at least equal to or even higher than those of Type C gears.

Figure 16 shows experimental results of the power losses of both Type C gears and corresponding low-loss gears. Enormous power loss savings of up to two-thirds can be achieved with low-loss gears. The given percentages of power loss reduction refer to the total power loss where higher bearing losses of low-loss gears are included because of the higher pressure angle. So, the pure load-dependent gear losses are even further reduced than the numbers suggest.

Besides power loss reduction, lower bulk and oil temperatures can also be achieved. Measurements during tests without lubrication showed a bulk temperature of 105°C for conventional gears where low-loss gears achieved 67°C. Also, its lifetime may be extended: Sample tests with coated gears—but without lubrication—showed that the coated gears had 15–20 times the load cycles of conventional gears before the coating was damaged.

Certainly, low-loss gears have some less favorable properties, including possible effects on design space and excitation level. Advantages like power loss reduction, temperature decrease and extreme lifetime extension make low-loss gears a viable option for many applications.


Conclusion

From the investigations shown in this report, the following main conclusions can be drawn:

- In a gearbox, bearing losses are subordinate to the losses in gears.
- In a gearbox, no-load losses are subordinate to the load-dependent losses at usual operating conditions. For operation at part-load or very high speeds, no-load losses may exceed the load-dependent losses.
- Load-dependent gear losses can be influenced by a range of

parameters, which either affect the load distribution along the path of contact or the coefficient of friction between the mating gear flanks.

- Conventional gears can be enhanced, but their power loss reduction is limited.
- With basically changed gear geometry, which optimizes the composition and interdependencies of all gear parameters, considerable loss reduction can be achieved.

Further investigations are necessary in the fields of load-carrying capacity and noise excitation properties of unconventional low-loss gear design. 

Acknowledgment

This paper contains results which were elaborated on the behalf of the sponsored project No. IPS-2001-80006 'Oil-free Powertrain' of the European Union EU. Therefore, we want to thank all participating industrial associations/ groupings:

VDMA—Verband Deutscher Maschinen- und Anlagenbau, Frankfurt, Germany;

FVA—Forschungsvereinigung Antriebstechnik, Frankfurt, Germany;

FVV—Forschungsvereinigung Verbrennungskraftmaschinen, Frankfurt, Germany;

FMS—Fachverband der Maschinen- und Stahlbauindustrie Österreichs, Wien, Austria;

Magosz—National Association of Hungarian Engineering Industry, Budapest, Hungary.

SST—Association of Manufacturers and Suppliers of Engineering Technique, Prague, Czech Republic;

AIA—Automotive Industry Association, Prague, Czech Republic.

References

1. Doleschel, A. EDV-Programm *WTplus*. FVA-Forschungsheft Nr. 625, 2001.
2. Eschmann, P., L. Hasbargen and K. Weigand. R. *Die Wälzlagerpraxis (Bearing Practice)*. Oldenbourg Verlag, München, 1978.
3. FAG. *Lagerkatalog (Bearing*

Catalog), 1999.

4. Gesellschaft für Tribologie. *Wälzlagerschmierung (Bearing Lubrication)*. GfT-Arbeitsblatt 3, 1993.

5. Haslinger, R., K. Salzgeber, and A. Wimmer. "Oil Free Powertrain – Work package 1.1. Analysis of Minimum Oil Requirements Considering Friction in Gears and Engines." EU-Project No. IPS-2001-80006. Final Report, 2003.

6. INA. *Nadellager, Zylinderlager (Needle and Roller Bearings)*, Katalog 306, 1995.

7. Mauz, W. "Hydraulische Verluste bei Tauch- und Einspritzschmierung von Zahnradgetrieben (Hydraulic Losses for Dip and Spray Lubricated Gears)." FVA-Forschungsvorhaben Nr. 44/III, Abschlussbericht, 1985.

8. Niemann, G. and H. Winter. *Maschinenelement (Machine Elements)*. Band 2, 2. Auflage, Springer-Verlag, Berlin, 1989.

9. Ohlendorf, H. *Verlustleistung und Erwärmung von Stirnrädern (Power Loss and Heat Generation in Cylindrical Gears)*. TH München, 1958.

10. Schinagl, S. RIKOR G, *EDV-Programm zur Ermittlung der Zahnflankenkorrekturen zum Ausgleich der lastbedingten Zahnverformungen (RIKOR G, Program Code for the Evaluation of Flank Corrections to Compensate Load Dependent Tooth Deformations)*. FVA-Forschungsheft Nr. 481, 2000. FVA-research report no. 481, 2000.)

11. Schlenk, L. "Größeneinfluss fressen" (Size Influence on Gear Scuffing). FVA-Forschungsvorhaben Nr. 166, Abschlussbericht, 1995. FVA-research project no. 166, final report, 1995.

12. SKF. *Walzlager (Anti-friction Bearings)*. Lagerkatalog, 1990.

13. Steingröver, K. FVA-Stirnradprogramm *STplus* (FVA-program code *STplus*). FVA-Forschungsheft Nr. 477, 2000.

14. Wimmer, A. "Konstruktive Einflüsse auf die lastabhängigen Verluste von Verzahnungen. (Geometrical Influences on Load Dependent Losses in Gears)". FVA-Forschungsheft Nr. 731, 2004.